 doi:10.20944/preprints201909.0225.v1

Article

Hybrid nanoelectronic-magnetic device with magnetoresistive effect for logic integrated platforms in spintronics

Ovidiu Crisan [1], Alina Daniela Crisan [2] and Catalin Luculescu [2,*]

[1] National Institute for Materials Physics, PO Box MG-7, 077125 Magurele, Romania;
[2] National Institute for Laser, Plasma and Radiation Physics , 077125 Magurele, Romania;
* Correspondence: ocrisan@yahoo.com;

Abstract: We propose a concept of hybrid nanoelectronic-magnetic device for logic integrated platforms made of magnetic core-shell nanoparticles deposited onto prepatterned Si (111) substrate with basic logic circuitry made of metallic conductive lines. The synthesis of magnetic material and the creation of nanoelectronic prepatterned interdigitated die is reported and its capabilities are demonstrated in terms of magnetotransport properties. The laser pyrolysis method is employed in order to synthesize magnetic core-shell Fe / FeC nanoparticles with sizes between 12 – 15 nm. Two different layouts of interdigitated die, prepatterned with logic capacity, have been conceived using e-beam lithography, with various geometries. The as-obtained structures are morphologically characterized by means of optical, scanning and transmission electron microscopies. As-synthesized core-shell nanoparticles have been magnetically characterized inasmuch as the hybrid device obtained by depositing centrifugated and dispersed core-shell nanoparticles from liquid carrier solutions. For the first time, a significant giant magnetoresistive (GMR) effect, of about 8% at 4.2 K, has been observed and measured for the hybrid architectured device made of Fe / FeC nanosized materials on pre-patterned interdigitated die. This opens possibilities for the use of such devices as arrays of nanosensors and in spintronic applications.

Keywords: magnetic nanoparticles; logic integrated platform; laser pyrolysis; nanosized materials;

1. Introduction

Among the most recent and innovative approaches for synthesis of advanced functional materials at a nanometric scale, nanoparticle organization has proven to be one of the most effective ways for obtaining mono-dispersed nanoparticles (NP's), dispersed onto extended areas [1-4]. Such arrays of dispersed NP, obtained by a simple and extremely cost effective procedure, may constitute the building blocks for complex-architecture nanostructures for applications in nanoelectronics, applications that uses spin manipulation, and for creation of devices with high added value. On the other hand, one of the newest sciences, related to spin manipulation in magnetic materials, is spintronics [5]. Spintronics utilizes the spin dependent scattering of conduction electrons caused by the direction and magnitude of spontaneous magnetization in magnetic-conductive two-phase materials, at a nanometric scale [6]. The effects exploited in such nanostructures are giant magnetoresistance GMR and spin dependent tunneling SDT [7]. The outstanding importance and novelty of these effects for an increased number of applications in nanotechnology, spintronics, nanoelectronics and in the magnetic heads industry, has been globally recognized by awarding the Nobel Prize for Physics 2007 to A. Fert and P. Grunberg for the discovery of GMR effect [8]. Materials that exhibit GMR effect are currently used in spin electronics as magnetic read heads, spin valves or tunnel junctions. GMR materials are generally made of conductive regions (films, grains), alternated with or separated by magnetic regions (films, grains). Spin reorientation in the magnetic regions due to application of a magnetic field, cause spin dependent scattering of conduction

Preprints (www.preprints.org) | NOT PEER-REVIEWED | Posted: 19 September 2019 doi:10.20944/preprints201909.0225.v1

electrons moving through material at the interface conductor/magnet. The presence of an applied magnetic field may be easily detected by the changes in the resistivity in the material, this being the main effect used in applications. By detection of the smallest changes in the magnetic field, that causes the change in resistance, the GMR materials may be used as magnetic sensors. Until now, exploitation of such effects have been limited to the case of thin films and multilayers [9,10], and to some limited extent, due to imperfect grain disposal, defects and grain boundaries, in nanogranular GMR alloys [1-16]. The first choice when it comes to the synthesis of NP's capable to self-organize into 2D arrays has been the colloidal chemistry [1-4,17]. Lately, besides the colloidal bimetallic core-shell NP's, another approach undertaken was to use surface-functionalized nanoclusters (NC's) obtained using a novel gas-stabilized cluster aggregation method [18]. Whereas the choice of colloidal core-shell NP's systems is limited by the composition of the organo-metallic precursors, used for the colloidal synthesis procedures, to only several bimetallic options (AgCo, FePt, FePd, CoPt, MnPt) the gas-phase aggregation method has the versatility of obtaining complex alloyed, core – multiple shells NC's with tightly controlled core size and shell thickness and, moreover, free choice of materials in the core and shells, from exchange bias Fe / Fe oxide [19] and Co / CoO [20] to Fe / Si luminescent clusters [21]. We propose in the current paper to create a hybrid architecture structure where a logic conditioned interdigitated die is used to support the magnetic nanomaterial and arrange it into a logic integrated platform and we demonstrate its functionality as spintronic and sensing device by detection of significant magnetoresistive signal along metallic conductive predefined interdigits.

2. Experimental

2.1. Logic conditioned interdigitated die

In order to prepare the logic conditioned interdigitated die for the hybrid architectures, Si(111) wafers have been used. A protective 500 nm oxide layer has been grown on top by baking the wafers in induction furnace at 1100°C. On the oxide layer a 20 nm thick Cr layer has been grown by e-beam evaporation. The layout of the polymer masks has been designed using Clewin software from WieWeb, The Netherlands. To completely cover the Si wafers, an alternate disposal of 2 different configurations has been considered. As a consequence, independent units of 4 x 4 mm covering a total area of 8 x 16 mm have been designed. The geometric configurations of the two layouts are presented in Figs. 1.

The layout 1 consists of 4 pads, 300 x 400 μm, connected through thin 50 μm conductive lines with 5 μm spacer which disconnects the interdigits.

The layout 2 contains parallel 2 μm thick lines separated by 5 μm spacer. The lines are connected to the large contact pads, on top and bottom of the figure. The as-designed mask has been made of PMMA photoresist.

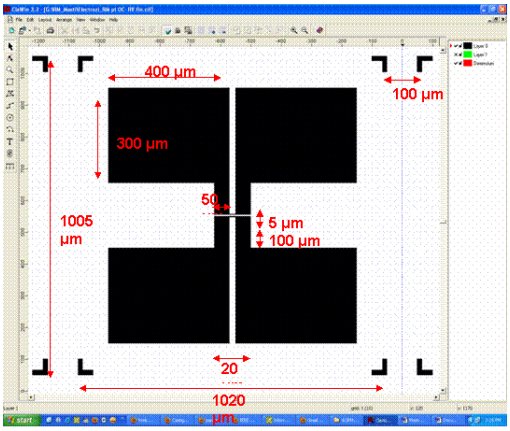

Fig. 1a: Mask for the layout 1. Pad size is shown in the figure.

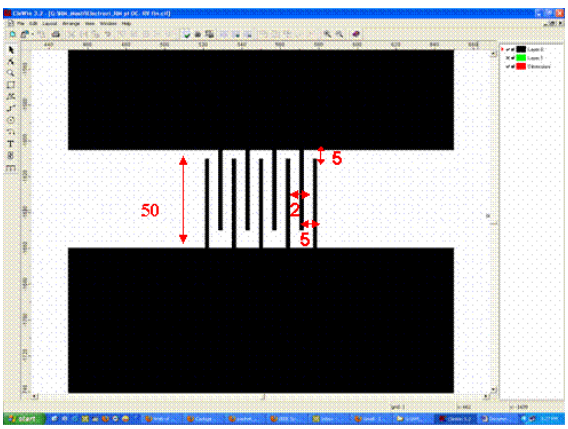

Fig. 1b: Mask for the layout 2. 2 μm parallel conductive lines are separated by a 5 μm spacer.

Preprints (www.preprints.org) | NOT PEER-REVIEWED | Posted: 19 September 2019 doi:10.20944/preprints201909.0225.v1

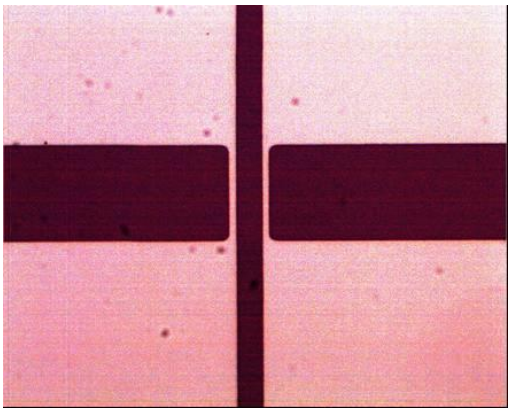

Fig. 2a: Optical image of the layout 1 masks.

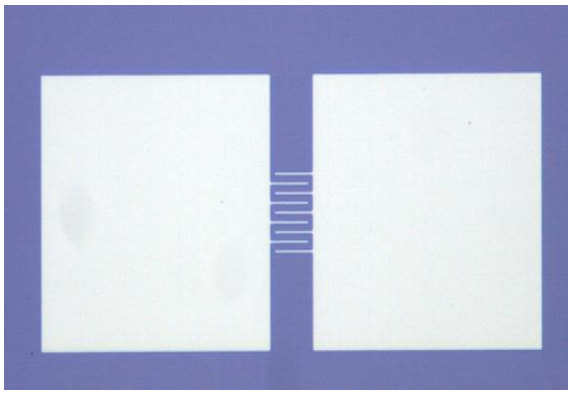

Fig. 2b: Optical image of the layout 2 masks.

The prepatterning has been performed using e-beam lithography. The metallic layer deposited onto the conductive lines was made of Cr-Au. After lift-off and corroding the metallic layer, a grid type configuration of interdigits, as in the layouts from Fig. 1, are obtained. The contact pads are 300 – 400 μm large, allowing thus enough room to make low resistivity (In) contacts for the magnetotransport and electric measurements.

Figs. 2 show optical microscopy images of the logic conditioned prepatterned dies. One can observe the uniformity and continuity of the metallic grid lines obtained after prepatterning. More detailed images of the whole prepatterned, logic conditioned interdigitated dies have been obtained using scanning electron microscopy (SEM) imaging (Figs. 3). The values determined on the SEM image are quite consistent with the mask-defined dimensions for the spacer and the conductive line respectively. For instance, in the Fig. 3b the size of the line is determined to be 1.8 microns, compared to the 2 microns, established by the mask layout, while the spacer size is determined to be 4.92 microns, compared to the 5 microns established by the mask layout.

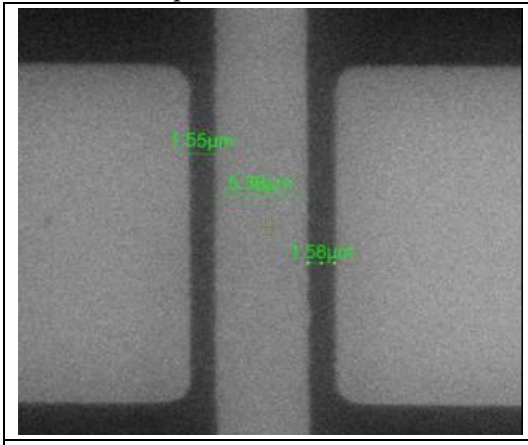

Fig. 3a: Scanning electron microscopy image of details of conductive line of mask with layout 1

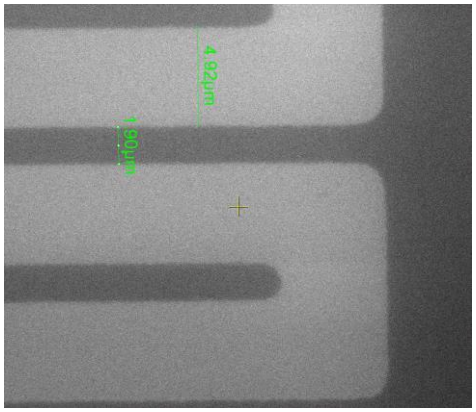

Fig. 3b: Scanning electron microscopy image of details of conductive line of mask with layout 2

2.1. Nanoparticles synthesis and characterization

The magnetic core-shell Fe/C nanoparticles have been obtained using laser pyrolysis technique. The home-made facility consists of a cross-shaped reaction chamber, a precursors input system, a CO_2 laser and the collecting chamber. The mixture of metallic precursors, in our case the $Fe(CO)_5$, and a sensitizer (ethylene – C_2H_4) is propelled together with a rare gas carrier (Ar) into the reaction chamber where the mixture is irradiated with the laser and ignites. The rare gas carrier flux drives the small solid particles, obtained after burning the gas mixture, into the collection chamber where the particles

Preprints (www.preprints.org) | NOT PEER-REVIEWED | Posted: 19 September 2019 doi:10.20944/preprints201909.0225.v1

are afterward scrapped off a filter and collected and dispersed into liquid carrier. The schematic of the preparation facility is provided in Fig. 4. The Fe:C stoichiometry is determined from adjusting the experimental parameters: the laser power and the $Fe(CO)_5$ / ethylene gas mixture ratio. To obtain stable suspensions the magnetic nanoparticles have been incorporated into suitable liquid carriers. We have considered as liquid carriers the chitosan and the natrium carboxymethyl cellulose (CMC). The actual concentration of magnetic nanoparticle in solution has been determined after successive cycles of dispersion / centrifugation of nanoparticles, and measurement of the absorption spectra using a Perkin-Elmer Lambda 950 spectrometer, however details about the dispersion can be found in a previous paper [22].

The transmission electron microscopy (TEM) imaging is used to observe the degree of dispersion of the nanoparticles, their morphology and periodicity, the uniformity of the dispersion. In the Fig. 5 TEM images of the Fe-C nanoparticles, before and after centrifugation are shown. It can be observed that Fe-C nanoparticles are obtained with a spherical shape, with an average size of about 13-15 nm. As-synthesized nanoparticles show agglomeration while after centrifugation the nanoparticles are much more isolated and better observed. High-resolution TEM image (Fig. 6) of the supernatant's nanoparticles indicates quite clearly the core-shell aspect of the FeC.

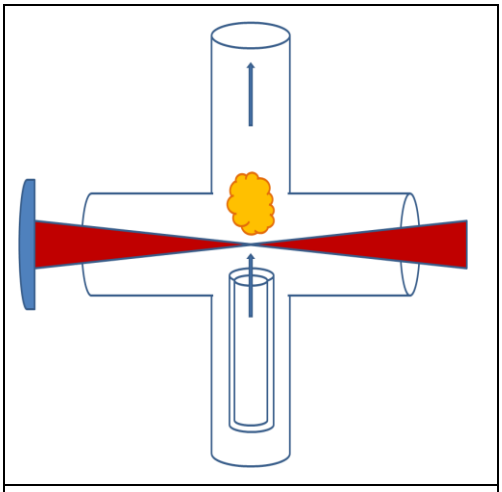

Fig. 4. Schematic of the reaction chamber of the laser pyrolysis facility

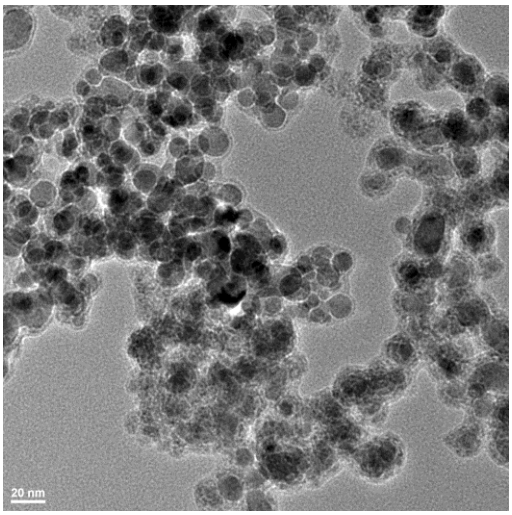

Fig. 5a : TEM image of Fe/ FeC nanoparticles before dispersion

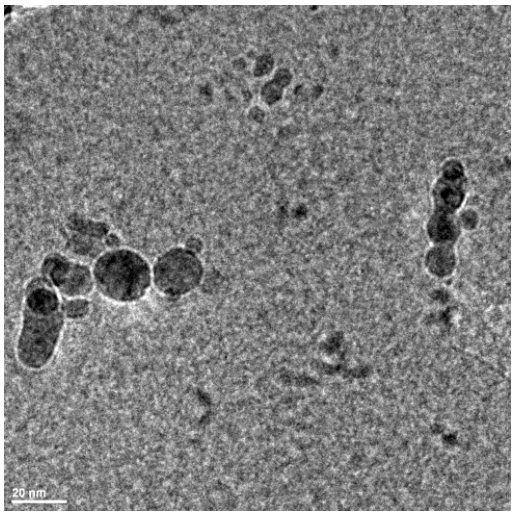

Fig. 5b: TEM image of Fe/ FeC nanoparticles after dispersion

Preprints (www.preprints.org) | NOT PEER-REVIEWED | Posted: 19 September 2019 doi:10.20944/preprints201909.0225.v1

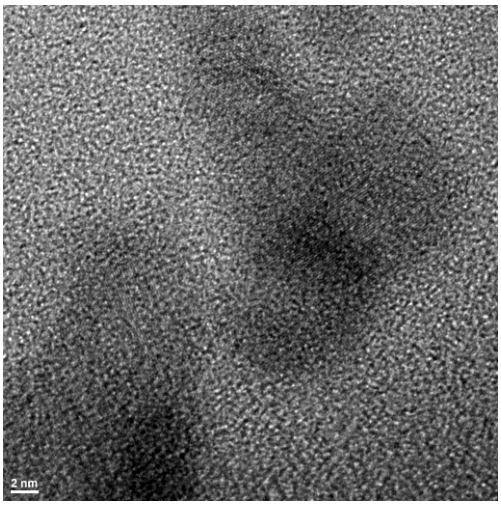

Fig. 6a: High-Resolution TEM image of Fe/ FeC as-synthesized nanoparticles

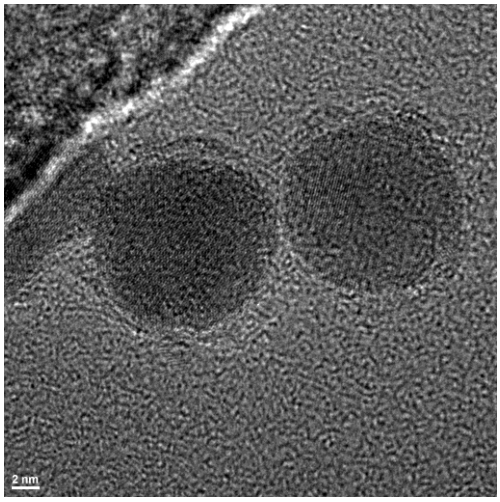

Fig. 6b: High-Resolution TEM image of Fe/ FeC nanoparticles in supernatant

3. Results and Discussion

3.1. Integration

The hybrid architectures have been subsequently obtained by deposition of the FeC nanoparticles solutions onto the logic conditioned prepatterned die. In order to achieve a regular and homogeneous dispersion, we have used a spin coater working in low vacuum (10^{-2} mbar) at 100 rpm. In the Fig. 7 the SEM images of the obtained hybrid structure with the nanoparticles deposited onto the logic conditioned device are shown. As we have used for deposition the supernatant nanoparticles solution, the concentration was quite low therefore the observed nanoparticles are organized mostly as traces along the conductive lines. It is worthwhile mentioning the tendency of the nanoparticles to organize at the edge of the conductive lines, the interface between the Si wafer substrate and the metallic line. Such behavior has been also observed in AgCo core-shell nanoparticles [23] deposited onto Si substrates.

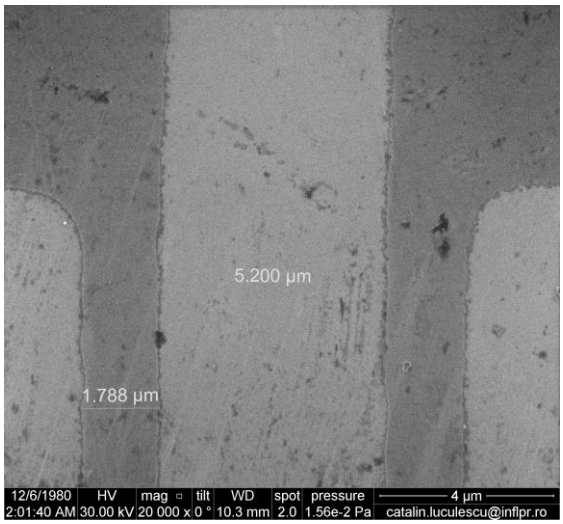

Fig. 7. Scanning electron microscopy images of the hybrid device obtained after deposition of NP solution onto the logic conditioned device (20000 x magnification)

Preprints (www.preprints.org) | NOT PEER-REVIEWED | Posted: 19 September 2019 doi:10.20944/preprints201909.0225.v1

3.2. Magnetic characterization

The hybrid architectures have been subsequently obtained by deposition of the FeC nanoparticles The Fe/FeC core-shell nanoparticles have been magnetically characterized using a Superconducting Quantum Interference Design SQUID facility, in applied magnetic field of up to 5 T. Such device is highly sensitive, having a 10^{-6} emu resolution in the determination of the magnetic moment, allowing thus investigations on highly diluted magnetic systems and magnetic fluids. Nanoparticles solutions dispersed in CMC centrifugated for 1h and 5h and in chitosan centrifugated for 1h have been measured in special capillaries. Figs. 8 show the hysteresis loops of the FeC core-shell nanoparticles obtained at 265K.

It can be seen that in the case of NP dispersed in CMC the behavior is of a soft magnetic material, which is typical for mono-phased materials based on Fe [24-28]. Magnetization rises sharply at very low applied fields and reaches saturation at around 500-1000 Oe applied field. The situation is similar for the two CMC dispersed NP solutions.

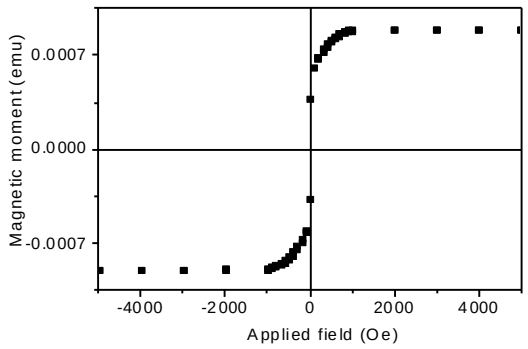

Fig. 8a: 265K Hysteresis loop of NP's dispersed in CMC centrifugated for 1h.

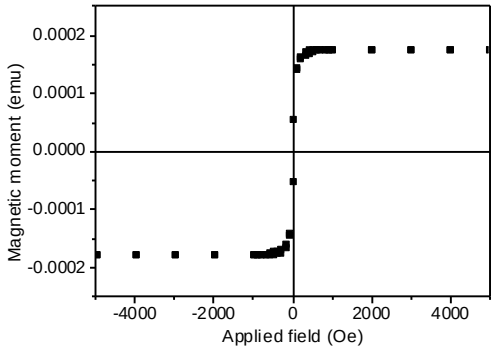

Fig. 8b: 265K Hysteresis loop of NP's dispersed in CMC centrifugated for 5h.

Preprints (www.preprints.org) | NOT PEER-REVIEWED | Posted: 19 September 2019 doi:10.20944/preprints201909.0225.v1

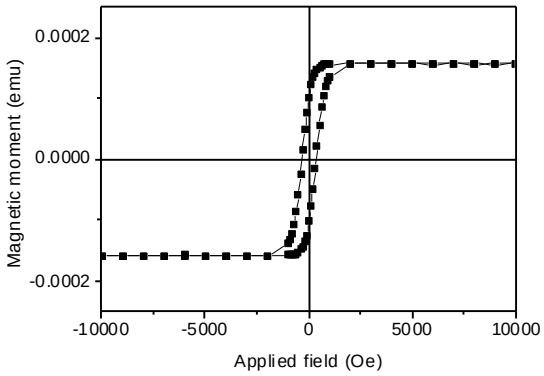

Fig. 8c: 265K Hysteresis loop of NP's dispersed in chitosan centrifugated for 1h.

A different situation is encountered though for the FeC NP dispersed in chitosan. A clear increase of the coercivity at 265K is observed for this sample (Fig. 8c) compared to the other ones. This increase of coercivity may signal the occurrence of pinning fields and spin freezing in magnetic configurations with linear domain walls. The spin reorientation transition towards a spin frozen state, that is proven to occur at 265K in the FeC nanoparticles dispersed in chitosan, has the advantage that it will eventually facilitate the detection of a high magnetoresistive signal, due to the spin-dependent electron transport along the conductive current lines – the logic conditioning – through the magnetic nanoparticles deposited onto these lines. In the case of a spin frozen magnetic configuration, this spin-dependent signal will be in phase and easier to detect in normal four-point-probe measurement configuration of the GMR.

3.3. Magnetic behavior of the hybrid structure

As mentioned before, the hybrid structure has been obtained by deposition of highly diluted NP solutions onto the prepatterned, logic conditioned,interdigitated die. The unit consists of repeated independent logic structures of 4 x 4 mm onto a total area of 8 x 16 mm. The conductive lines are in such way configured / preconditioned as to allow either a four-point-probe measurement protocol (4 pads) or a two-point-probe protocol (2 pads, see Figs. 1, 2). In order to obtain the magnetic features of the whole hybrid structure, we have performed magnetization measurements using SQUID magnetometry at 300K. The resulting hysteresis loop of the hybrid structure is shown in Figure 9.

A similar hysteresis loop as in the case of as-synthesized nanoparticles is obtained. A value of about 2.5 x 10^{-3} emu has been obtained for the magnetic moment. As the density of the deposited magnetic nanoparticles is well below 1 monolayer of nanoparticles, this quite high value of saturation magnetization is very promising and shows potential for obtaining magnetoresistive signal and good perspectives in view of potential applications in spintronics.

Preprints (www.preprints.org) | NOT PEER-REVIEWED | Posted: 19 September 2019 doi:10.20944/preprints201909.0225.v1

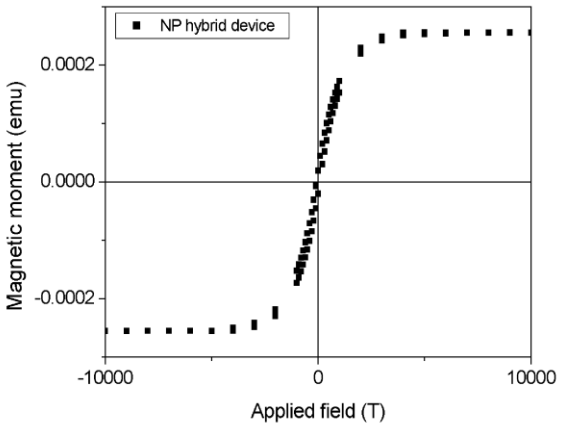

Fig. 9: 300K Hysteresis loop of hybrid architecture obtained by deposition of NP's dispersed in chitosan onto the logic conditioned interdigitated die

3.4. Magnetotransport behavior of the hybrid structure

Magnetoresistive measurements have been performed on the surface of the hybrid structure using a Physical Property Measurement System PPMS 5 in four-point-probe setup. The facility allows measurements from 1.2 K up to 300K in an applied field of up to 5.5 T. We have chosen two different measurement geometries: the conductivity in-plane (CIP) using only two pads and the cross-over geometry, using all 4 pads. For the cross-over configuration, we have chosen the unit having the layout 2, with 4, 300 microns wide, pads, and 1.5 microns wide conductive lines. Layout 1 with two pads was used for measuring the magnetoresistance in CIP geometry. Both measurements have shown variations of the resistivity with the applied field, thus proving that such hybrid structure may be effective in applications as magnetic sensors.

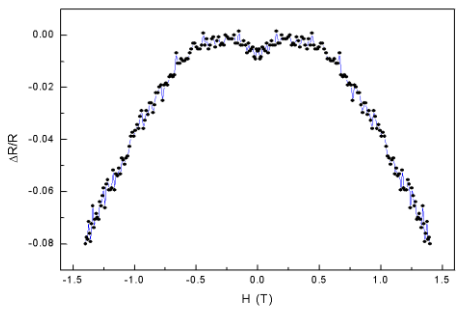

Fig. 10a: GMR response of the hybrid structure in positive and negative applied field at 4.2 K, in CIP configuration.

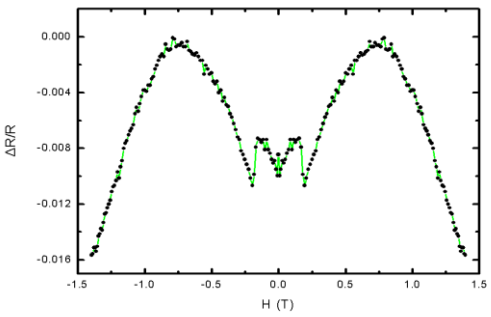

Fig. 10b: GMR response of the hybrid structure in positive and negative applied field at 4.2 K, in cross-over configuration.

Figs. 10 show the magnetoresistive curves as a function of the applied field, recorded at 4.2 K, in CIP and cross-over configuration, respectively. The magnetoresistance is given by the ΔR/R ratio defined as:

 doi:10.20944/preprints201909.0225.v1

$$\frac{\Delta R}{R}(T,H) = \frac{R(T,H) - R(0)}{R(0)} \quad (1)$$

where R(T,H) is the resistance at a given H of the applied field and at a given temperature T and R(0) is the resistance at the temperature T in the absence of the applied field.

It can be seen for both configurations the symmetry of ΔR/R branches when the applied field is positive or negative. There is no hysteresis of the magnetoresistance. In both cases the GMR response is not saturated at 1.5 T, being thus possible to obtain an even higher GMR response if the applied field is increased. In the CIP configuration the hybrid structure shows the highest GMR, of about 8% at 4.2 K. It is a significantly high GMR value that may allow the use of such hybrid structures as magnetic GMR sensors. In the cross-over configuration the GMR effect recorded is only 1.6% at 4.2 K, due mainly to the purely resistive component of the electron transport. It is widely known that the GMR effect is given by the spin dependent scattering of the conduction electron at the magnetic / conductive interface. But a non-negligible component is given also by the scattering inside the magnetic nanograins. It appears that a higher number of conductive / magnetic interfaces correlated to lowered nanograin sizes is an essential conditions to minimize the intra-particulate scattering and consequently to improve the GMR response.

4. Conclusions

A combined approach of nanoelectronics methods and chemical vapour precipitation routes has been undertaken in order to build a hybrid architectured logic device of magnetic core-shell nanoparticles deposed onto prepatterned, logic conditioned, interdigitated die. A Si (111) substrate has been prepatterned with 2 layouts of repeated logic conditioned independent units of parallel conductive metallic lines separated by Si spacer. The laser pyrolysis method has been used to synthesize core-shell magnetic Fe / FeC nanoparticles from metal-organic precursors, with controlled particle sizes of the order of 12-15 nm. Extensive scanning and transmission electron microscopy studies were undertaken in order to image the shape, size and morphology of the core-shell nanoparticles, as well as the periodicity and homogeneity of the dispersion of nanoparticles. The as-synthesized nanoparticles have been dispersed into CMC and chitosan liquid carriers by centrifugation. Magnetic behavior of the nanoparticles solutions have been measured using SQUID magnetometry and it was shown to exhibit a soft magnetic behavior with large saturation magnetization. In the case of chitosan liquid carrier, an increase of the coercivity has been observed and attributed to a spin reorientation phenomenon. The as-obtained solutions have been deposited by spin coating onto the prepatterned logic conditioned Si substrate. The hybrid logic device thus obtained has been also magnetically characterized and its magnetotransport electron properties have been obtained. It has been shown that such hybrid architectured structure exhibits a significant giant magnetoresistance effect of about 8% at 4.2 K. This makes such hybrid structures suitable for advanced applications as logic integrated platforms of nanosensors.

Funding: This research was funded by Romanian Ministry of Research through grant Ideas 187 / 2017; PN-III-P4-ID-PCE-2016-0833.

References

1. S. Sun, C. B. Murray, D. Weller, L. Folks, A. Moser, Science **2000**, *287*, 1989-1992
2. S. Sun and C.B. Murray, J. Appl. Phys. **1999**, *85*, 4325-4327,.
3. M. Chen and D.E. Nikles, J. Appl. Phys. , **2002** *91*: 8477-8479.
4. H. Zeng, S. Sun, T.S. Vedantam, J.P. Liu, Z.R. Dai, Z.L. Wang, Appl. Phys. Lett. **2002** *80*: 2583-2585,.

5. T. Shinjo, Nanomagnetism and spintronics, Elsevier Science, New York, **2009**.
6. I. Zutic, J. Fabian, S. Das Sarma, Rev. Mod. Phys. **2004** *76*: 323-409,.
7. J.S. Moodera, G. Mathon, J. Magn. Magn. Mater. **1999** *200*: 248-255,.
8. M.N. Baibich, J.M. Broto, A. Fert, F. Nguyen van Dau, F. Petroff, P. Etienne, G. Creuzet, A. Friederich, J. Chazelas, Phys. Rev. Lett. **1988**, *61*:2472-2475,.
9. S.K. Mishra et al, Phys. Rev. B **2010** *81*: 212404,.
10. P. Vlaic, E. Burzo, J. Appl. Phys. **2011** *109*: 063724.
11. O. Crisan et al., J. Magn. Magn. Mater. **1999** *195*: 428-436,.
12. A.D. Crisan, O. Crisan, Mater. Sci. Technol. **2012** *28* 460-466
13. A.D. Crisan, O. Crisan, J. Phys. D: Appl. Phys. **2011** *44* 365002
14. O. Crisan, A.D. Crisan, J. Alloys & Compd. **2011**, *509* 6522-6527
15. O. Crisan, A.D. Crisan, J. Optoelectron. Adv. Mater. **2010** *12* 184-192
16. A.D. Crisan, J. Optoelectron. Adv. Mater. **2010** *12* 250-256
17. A.D. Crisan, M. Angelakeris, K. Simeonidis, I. Tsiaoussis, O. Crisan, Solid State Sci. **2010** *12*: 1907-1911,.
18. O. Crisan, K. von Haeften, C. Binns, A.M. Ellis, Nanotechnology **2008** *19*: 505602,.
19. O. Crisan, K. von Haeften, C. Binns, A.M. Ellis, J. Nanopart. Res. **2008** *10*: 193-199,.
20. J.A. Gonzalez, J.P Andres, J.A. De Toro, P. Muniz, T. Munoz, O. Crisan, C. Binns, J.M. Riveiro, J. Nanopart. Res. **2009** *11*: 2105-2011,.
21. K. von Haeften, C. Binns, A. Brewer, O. Crisan, P.B. Howes, M.P. Lowe, C. Sibbley-Allen, S.C. Thornton, Eur Phys J D **2009** *52*: 11-14.
22. I. Morjan, F. Dumitrache, R. Alexandrescu, C. Fleaca, R. Birjega, C.R. Luculescu, I. Soare, E. Dutu, G. Filoti, V. Kuncser, G. Prodan, N.C. Popa, L. Vekas, Adv. Powd. Technol. **2012** *23*: 88-96,.
23. O. Crisan, M. Angelakeris, M. Nogues, Th. Kehagias, Ph. Komninou, N. Sobal, M. Giersig, N.K. Flevaris, J. Magn. Magn. Mater. **2004** *272*: E1253-E1254,.
24. V.R. Reddy, O. Crisan, A. Gupta, V. Kuncser, A.Banerjee, Thin Solid Films **2012** *520* 2184-2189
25. O. Crisan, J.M. Le Breton, G. Filoti, Sensors and Actuators A **2003** *106*: 246-250,.
26. M. Rosenberg, V. Kuncser, O. Crisan, A. Hernando, E. Navarro, G. Filoti, J. Magn. Magn. Mater. **1998** *177*: 135-136,.
27. O. Crisan, J.M. Le Breton, M. Nogues, F. Machizaud, G. Filoti, J. Phys.: Condensed Matter **2002** *14* : 12599-12609,.
28. M. Seqqat, M. Nogues, O. Crisan, V. Kuncser, L. Cristea, A. Jianu, G. Filoti, J.L. Dormann, D. Sayah, M. Godinho, J. Magn. Magn. Mater. **1996** *157*: 225-226,.